INSTITUT DE FRANCE
Académie des sciences

Comptes Rendus
Mathématique

Damiano Lombardi, Yvon Maday and Lydie Uro

Fast semi-automatic segmentation based on reduced basis

Volume 358, issue 9-10 (2020), p. 981-987

Published online: 5 January 2021

https://doi.org/10.5802/crmath.89

Les Comptes Rendus. Mathématique *sont membres du Centre Mersenne pour l'édition scientifique ouverte*
www.centre-mersenne.org
e-ISSN : 1778-3569

Comptes Rendus
Mathématique
2020, 358, nº 9-10, p. 981-987
https://doi.org/10.5802/crmath.89

Numerical Analysis / *Analyse numérique*

Fast semi-automatic segmentation based on reduced basis

Méthode de segmentation semi-automatique fondée sur une base réduite

Damiano Lombardi [a], **Yvon Maday** [b] **and Lydie Uro** [*, c]

[a] COMMEDIA, Inria Paris, 2 rue Simone Iff, 75012, Paris, et Sorbonne Université, Laboratoire Jacques-Louis Lions (LJLL), F-75005 Paris, France

[b] Sorbonne Université, CNRS, Université de Paris, Laboratoire Jacques-Louis Lions (LJLL), F-75005 Paris et Institut Universitaire de France, France

[c] Sorbonne Université, Institut des Sciences du Calcul et des Données (ISCD), F-75005 Paris, France

E-mails: damiano.lombardi@inria.fr (D. Lombardi), maday@ann.jussieu.fr (Y. Maday), lydie.uro@sorbonne-universite.fr (L. Uro)

Abstract. This note adresses the following segmentation problem in medical imaging: minimize expert intervention for semi-automatic segmentation process. Using a reduced basis, we have an a priori knowledge of the objet we want to identify on the images, like a muscle on a CT-Scan. We just have to identify the coefficients associated to the object of interest in the reduced basis, by solving a linear system taking as input the coordinates of some selected points in the image. An example implemented in 2D is shown. This method is independent of the grayscale of the image, and can therefore be applied to all objects and images.

Résumé. Nous présentons ici une méthode de segmentation d'imagerie médicale semi-automatique minimisant l'intervention d'un expert. A l'aide d'une base réduite, nous connaissons a priori la forme de l'objet à identifier sur les images, comme un muscle sur un scanner. Il suffit d'identifier les coefficients associés à l'objet d'intérêt dans la base réduite, via la résolution d'un système linéaire prenant en entrée les coordonnées de quelques points sélectionnés sur l'image. Un exemple implémenté en 2D est proposé. Cette méthode est indépendante des niveaux de gris de l'image, et peut donc être appliquée sur tous objets et toutes imageries.

Manuscript received 11th October 2019, revised 26th May 2020, accepted 24th June 2020.

* Corresponding author.

1. Introduction

One of the recurring and time consuming challenges in medical imaging is the segmentation of parts of interest. Segmentation is the process of dividing a medical image into distinct anatomical regions [9]. This has been for years the effort of specialists and it is quite time consuming. Beyond the specifics takes of each particular application, the general issue is to find a way to identify automatically an anatomical region of interest in order to speed up the process. When the contrast is high enough (e.g. for bones, or between bones and tissues) automatic segmentation is quite efficient and various methods have been proposed and implemented [6,11,16]. Likewise for anatomical major organs like the brain or the heart [1,3,14]. On the contrary, when the contrast is not high enough (e.g. segmentation between different soft tissues on CT scans) the most common imaging modalities fail and there are very few approaches available.

Understandably enough, most of the current segmentation methods are based on the gray scale which can let experts easily differentiate 2 objects [10]. Several classifications of those methods exit, we can cite [15] for an overview. We limit ourselves to mentioning here a few approaches, for some more detail surveys we can look at [4, 7] for example.

Thresholding and edge detection are two very common approach used for image segmentation [8, 12]. They are simple and effective approaches to segment anatomical details featured by high contrast, as, for instance, the bones (that appear as light objects on dark background). However, it is more challenging for the detection of objects that do not have a marked gray scale signature, as muscles. We can also cite the region based method [8]. Three other types of process can be mentionned here: deformable models [4], atlas guided [5] and all the approaches dealing with artificial intelligence, which has recently been blooming up in the field of medical image segmentation [13, 15].

We propose here to develop a model based semi-automated method to help segmentation, which have most in common with the three last types of methods cited above. In particular, the shape of the object of interest is represented by an elastic deformation field of a reference configuration. A reduced basis representation of the object of interest is introduced, that exploits an a posteriori knowledge of a database of available segmentations. Given an image to be segmented, the elastic deformation field can be approximated as a linear combination of a small number of modes. This provides, in turn, a powerful regularisation method and a significant speed-up of the procedure since only few apropriate points need to be selected by the user in order to define the field. We can find a similar idea in [2], but with a probabilistic point of view, and where all the modes of the PCA are used as a regularisation and not as a dimentional reduction.

The proposed method is complementary to the ones exposed before, first because it requires some preliminary segmentations to "build" the reduced basis, and second because it can be used indifferently on CT and MR image for any type of object, even the ones difficult to identify like soft tissues on a CT.

The paper is structured as follows: in Section 2, the problem and the notations are presented. Then, in Section 3 some numerical experiments are detailed.

2. Notation and problem setting.

Most medical imaging modalities produce a gray-scale image, i.e. a function defined over a subset of $\mathbb{R}^2$ (or $\mathbb{R}^3$ for 3D imaging), $f : \mathbb{R}^2 \to [0,1]$ associating a scalar value to each point of the space (denoted later on by $x = (x_1, x_2)$ (or by $x = (x_1, x_2, x_3)$ in 3D)). After a manual segmentation of a region of interest is performed, it is possible to model this region by using an elastic morphing that maps a reference object: e.g. an ellipse in $\mathbb{R}^2$ (or an ellipsoid in $\mathbb{R}^3$) onto the boundary of the

two-dimensional (or three-dimensional) segmented region. In the present work, for the sake of simplicity, we will restrict to two-dimensional configurations. Having a collection of segmented objects (belonging to a coherent family) is equivalent to having a set of 2D elastic displacement fields mapping a same (reference) ellipse into the different segmented objects.

Let us assume that the reference configuration is an ellipse $E \subset \mathbb{R}^2$; a point $\boldsymbol{\xi} \in \partial E$ is mapped through a displacement field into a point $\mathbf{x} \in \partial F \subset \mathbb{R}^2$, where F is the boundary of the segmented object. It holds:

$$\begin{cases} Id + u : E \to F \\ \boldsymbol{\xi} \mapsto \mathbf{x} = \boldsymbol{\xi} + u(\boldsymbol{\xi}), \end{cases} \tag{1}$$

and $u \in H^1(E)$.

From an acquired database[1] consisting of $N \in \mathbb{N}^*$ such elastic displacements : $\mathscr{D} = \{u^{(1)}, \ldots, u^N\}$, let us assume that a set of $n \in \mathbb{N}^*$, with $n \leq N$, Proper Orthogonal Decomposition (POD) modes is extracted:

$$\varphi_i : E \to F,\ i = 1, \ldots, n. \tag{2}$$

When a new image to be segmented is available, the unknown elastic displacement mapping the reference configuration onto the image can be approximated by using the POD basis as follows:

$$u \approx u_n = \sum_{i=1}^{n} \alpha_i \varphi_i. \tag{3}$$

The goal is to find the coefficients α_i in such a way that the reference ellipse, mapped by the displacement field $Id + u_n$ is as close as possible to the actual image, hence providing an already good guess for the segmentation. In order to identify the coefficients α_i a semi-automated procedure is devised. The image does not correspond, in general, to the reference configuration (this would be the case in which $\alpha_i = 0,\ \forall\ i$). A number of $m \in \mathbb{N}^*$ points $\mathbf{x}^{(j)} \in \partial F$ is selected in which there is a discrepancy between the actual image and the reference configuration. Each of these points correspond to an equation for the displacement field: there exists a $\boldsymbol{\xi}_*^{(j)} \in \partial E$ such that:

$$\mathbf{x}^{(j)} = \boldsymbol{\xi}_*^{(j)} + \sum_{i=1}^{n} \alpha_i \varphi_i\left(\boldsymbol{\xi}_*^{(j)}\right),\ j = 1, \ldots, m. \tag{4}$$

This is a non-linear system of equations in the variables $\alpha_i, \boldsymbol{\xi}_*^{(j)}$; however, if the points $\boldsymbol{\xi}_*^{(j)}$ are known, this system is a linear system of equations for the coefficients α_i. In the present work, the points $\boldsymbol{\xi}_*^{(j)}$ are chosen as the ones minimising the distance to the point $x^{(j)}$[2]:

$$\boldsymbol{\xi}_*^{(j)} = \underset{\boldsymbol{\xi} \in E}{\arg\min} \left\| \mathbf{x}^{(j)} - \boldsymbol{\xi} \right\|_{\ell^2}^2,\ j = 1, \ldots, m. \tag{5}$$

This corresponds to a regularisation for the solution of the non-linear system Equation (4). The linear system to be solved reads:

$$\Phi \alpha = d, \tag{6}$$

$$\Phi_{jik} = \varphi_{i,k}\left(\boldsymbol{\xi}_*^{(j)}\right), \tag{7}$$

$$d_{j,k} = \mathbf{x}_k^{(j)} - \boldsymbol{\xi}_{*k}^{(j)}, \tag{8}$$

where Φ is a tensor, assumed to be of maximal rank (remember that it is constructed from POD vectorial modes). Of course, as soon as $m \geq n$, the system is solved in a least-square sense, and admits a unique solution. When discretising and solving this system, the following choices are

[1] This database is assumed to be large enough to represent well the full coherent family we are interested in.

[2] Remark that this point might not be unique.

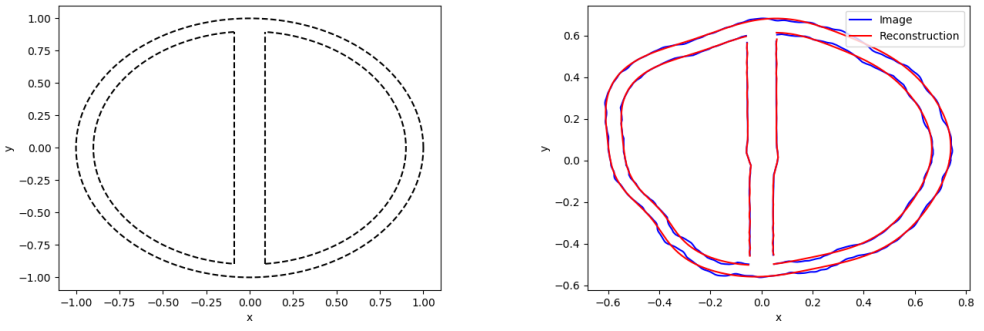

(a) (b)

Figure 1. Test case presented in Section 3: (a) Reference configuration (b) an image and its reconstruction.

made. The minimisation step described by Equation (5) is solved by using a nearest neighbor algorithm that, among the points of the discretised ∂E selects the one which is closest to a given $\mathbf{x}^{(j)}$. Then, the vector system in Equation (6) is unfolded and solved by using a rank revealing QR decomposition.

3. Numerical Experiments

In this section, some numerical experiments are shown on a simple 2D test case to assess the performances of the proposed semi-automated segmentation approach. The reference configuration, depicted in Figure 1.a), is a unit circle, divided into two semicircles. The images are defined by deforming this configuration by a parameter dependent field, generated as follows: The displacement of each point on the reference circle is normal to the circle and constructed by summing the set of $N_h \in \mathbb{N}^*$ harmonics (eigenfunctions of the Laplace–Beltrami operator), scaled with a parameter dependant coefficient : let the undeformed configuration points be denoted by $\xi \in \mathbb{R}^2$, $r = \|\xi\|_2 \leq 1$, $\vartheta \in [0, 2\pi]$ (i.e. $\xi_1 = r\cos(\vartheta)$, $\xi_2 = r\sin(\vartheta)$, the unit vector in the radial direction be denoted by $\widehat{e}_r$ and the displacement providing the deformed image configuration be $x \in \mathbb{R}^2$:

$$x = X(\xi) = \xi + r\left(\sum_{j=1}^{N_h} \alpha_j (j+1)^{-\beta}\right)\widehat{e}_r, \tag{9}$$

where $\alpha_j = \alpha_j(\mu)$, have an amplitude which decreases as a power law of the harmonics numbers: $(j+1)^{-\beta}$ with $\beta = 1.5$, and μ is a parameter that identifies each image.

Consider the following radial displacement, depending upon the parameter $\boldsymbol{\mu} \in [0,1]^2$. The harmonics coefficients are chosen according to the following expression:

$$\alpha_j = \frac{A}{j^2}\left[\sin\left(2\pi j\sqrt{\mu_1}\right) + \cos\left(2\pi j\sqrt{\mu_2}\right)\right],$$

In the present work $K = 100$ harmonics are used to generate the displacement fields. A set of $N = 100$ uniformly distributed in $[0,1]^2$ samples of the parameter μ are taken, and, for each, the radial displacement is constructed. The POD basis was computed. The singular value decay is shown in Figure 2.a, exhibiting a faster decay when compared to the one typical of the spherical harmonics for a given regularity.

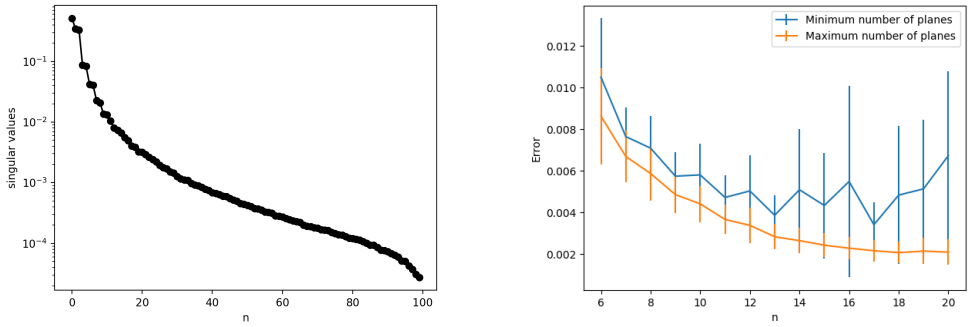

(a) (b)

Figure 2. Test case presented in Section 3: (a) Decrease of singular values with POD parametrisation (b) Error mean and standard deviation.

Remark that the displacement is purely radial and that the center of the reference circle $r = 0$ does not move. This corresponds to the case where the various anatomic regions that have been segmented are "aligned" and properly scaled. Furthermore, given this way of building a database of elastic displacements, the POD modes reduce to a set of vector displacements in the radial direction whose intensity is given by the value of the harmonics. The discretised shape is built by discretising uniformly the interval ϑ using $N_\vartheta = 512$ points.

The image (the deformation of the reference shape) is cut by $N_p \in \mathbb{N}^*$ horizontal planes, uniformly distributed on the image, to mimic a medical exam like CT or MRI which are sliced. Each plane intersects the outer boundary of the object in two points ($m = 2N_p$), each of which corresponding to one of the halves of the deformed circle. These points provide an equation for the displacement field to be approximated by using the POD modes.

Several numerical experiments are made to assess the performances of the proposed reconstruction method, by varying the number of modes and the number of cutting planes used. In particular, the number of modes used varied from $n = 6$ to $n = 20$ and, for each choice the number of planes was varied from the minimal number of planes needed to have a square system $n \leq m$ to $m = 2n$. In Figure 1.b) an example of reconstruction is proposed, when the image was produced by using $N_h = 100$ harmonics, $n = 20$, $m = 80$. The result is quite precise, all the details of the image are well represented, whether it is the outer edge where points are selected or the edge of the inner hemicycles where no points are selected.

The reconstruction errors are shown in Figure 2.b for a population of 100 target displacements (that do not belong to the database used to construct the POD modes). The errors are measured in ℓ^2 norm with respect to the discretised images. The average error and standard deviation are shown when the minimal number of planes and the maximum number of planes are used. In general, the errors are compatible with the ones considered as compatible with realistic applications. When the minimum number of planes is used a stability issue can be seen when a large number of modes is used and the standard deviation is quite large. On the contrary, when $N_p = 2n$ (orange), the lack of stability is delayed, the errors decrease and the standard deviation is much smaller, reaching a minimum for $n = 17$.

4. Conclusions and Perspectives.

In the present work a semi-automated reconstruction method is proposed to help the segmentation of anatomical details in the cases in which the contrast is not enough to use fully automated techniques. The method is based on the use of a reduced basis to approximate an elastic displacement mapping a reference configuration into the actual shapes of the anatomical details of interest. The method uses a nearest neighbors optimisation procedure coupled to a least square approach to solve the problem. A 2D test case is proposed to mimic realistic applications and assess the performances of the method. A set of synthetic generated images was used and the error of the numerical experiments showed that the proposed approach can lead to a viable tool. In this respect, further investigations are mandatory both from the theoretical and applied point of view. In particular a systematic error analysis will be carried out and more realistic tests will be performed, in 3D configuration and by taking the noise and the other experimental error sources into account.

Especially in 3D, several challenges are added to those described above, especially in the case of a real application. The first one is the constitution of the manual segmentation database: it takes time and requires the intervention of an anatomist expert at first. However, the idea is that we can, very quickly in this acquisition process, by the very approach of reduction, propose a first phantom that requires only a few corrections and saves a lot of time while continuing to feed the database. In addition, the mapping of the points would remain assured by the same idea as in 2D from a deformed reference configuration. However, instead of using a nearest neighbor algorithm, we will opt to define a probability density for each point in the point cloud of the corresponding dataset. In a second step, it is planned to replace the POD by a greedy algorithm, to increase the robustness.

References

[1] S. Bao, A. C. S. Chung, "Multi-scale structured cnn with label consistency for brain mr image segmentation", *Comput. Methods Biomech. Biomed. Eng. Imaging. Vis.* **6** (2018), no. 1, p. 113–117.

[2] F. Bernard, L. Salamanca, J. Thunberg, A. Tack, D. Jentsch, H. Lamecker, S. Zachow, F. Hertel, J. Goncalves, P. Gemmar, "Shape-aware surface reconstruction from sparse 3d point-clouds", *Med. Image Anal.* **38** (2017), p. 77-89.

[3] A. de Brebisson, G. Montana, "Deep neural networks for anatomical brain segmentation", in *Proceedings of the IEEE Conference on Computer Vision and Pattern Recognition Workshops*, Computer Vision Foundation, 2015, p. 20-28.

[4] T. Heimann, H.-P. Meinzer, "Statistical shape models for 3d medical image segmentation: a review", *Med Image Anal* **13** (2009), no. 4, p. 543-563.

[5] J. E. Iglesias, M. R. Sabuncu, "Multi-atlas segmentation of biomedical images: a survey", *Med Image Anal* **24** (2015), no. 1, p. 205-219.

[6] Y. Kang, K. Engelke, W. A. Kalender, "A new accurate and precise 3-d segmentation method for skeletal structures in volumetric ct data", *IEEE transactions on medical imaging* **22** (2003), no. 5, p. 586-598.

[7] G. Litjens, T. Kooi, B. E. Bejnordi, A. A. A. Setio, F. Ciompi, M. Ghafoorian, J. A. Van Der Laak, B. Van Ginneken, C. I. Sánchez, "A survey on deep learning in medical image analysis", *Med. Image Anal.* **42** (2017), p. 60-88.

[8] A. M. López, F. Lumbreras, J. Serrat, J. J. Villanueva, "Evaluation of methods for ridge and valley detection", *IEEE Trans. Pattern Anal. Mach. Intell.* **21** (1999), no. 4, p. 327-335.

[9] D. L. Pham, C. Xu, J. L. Prince, "Current methods in medical image segmentation", *Annu Rev Biomed Eng* **2** (2000), no. 1, p. 315-337.

[10] ———, "Current methods in medical image segmentation", *Annu Rev Biomed Eng* **2** (2000), no. 1, p. 315-337.

[11] M. S. M. Rahim, A. Norouzi, A. Rehman, T. Saba, "3d bones segmentation based on ct images visualization", *Biomedical Research* **28** (2017), no. 8, p. 3641-3644.

[12] N. Ramesh, J.-H. Yoo, I. Sethi, "Thresholding based on histogram approximation", *IEE Proceedings-Vision, Image and Signal Processing* **142** (1995), no. 5, p. 271-279.

[13] N. Sharma, L. M. Aggarwal, "Automated medical image segmentation techniques", *J. Med. Phys.* **35** (2010), no. 1, p. 3-14.

[14] T. S. Spisz, I. Bankman, *Handbook of medical imaging*, Academic Press, 2000.

[15] D. J. Withey, Z. J. Koles, "Medical image segmentation: Methods and software", in *2007 Joint Meeting of the 6th International Symposium on Noninvasive Functional Source Imaging of the Brain and Heart and the International Conference on Functional Biomedical Imaging*, IEEE, 2007, p. 140-143.

[16] J. Zhang, C.-H. Yan, C.-K. Chui, S.-H. Ong, "Fast segmentation of bone in ct images using 3d adaptive thresholding", *Computers in biology and medicine* **40** (2010), no. 2, p. 231-236.